MSUCL-934
McGill/94-44

Higher excitations of ω and ϕ in dilepton spectra

Kevin Haglin*
National Superconducting Cyclotron Laboratory, Michigan State University
East Lansing, Michigan 48824–1321

Charles Gale†
Physics Department, McGill University, 3600 University St., Montréal, Québec, H3A 2T8, Canada

(February 9, 2008)

Abstract

We consider lepton pair production via two-hadron annihilation through various isoscalar vector mesons within hot, baryon-free matter. This is tantamount to constructing effective form factors which we model using a vector-meson-dominance approach and compare with experiment. In particular, we consider the reactions $\pi\rho \to e^+e^-$ and $\bar{K}K^*(892)$ + c.c.$\to e^+e^-$. We find that $\omega(1390)$ and $\phi(1680)$ are visible in the mass spectrum for the thermal production rate above the $\pi^+\pi^- \to e^+e^-$ tail and even above the $\pi a_1 \to e^+e^-$ results—both of which were considered important in their respective mass regions.

PACS numbers: 25.75.+r, 12.38.Mh, 13.75.Lb

I. INTRODUCTION

Production of dileptons in high-energy heavy-ion collisions continues to be studied actively since it is hoped that such signals might be useful in discriminating prehadronic or quantum chromodynamic (QCD) plasma formation from ordinary hadronic matter. The possible success depends on having a reasonably complete picture of both plasma and hadronic phases. Crossover from one to the other is expected for a critical temperature in the neighborhood of 200 MeV and near this boundary the hadronic matter will be populated by many species of strange and nonstrange mesons. However, to get a rough idea about this phase of matter one typically used a simple pion-gas approximation. In terms of dilepton spectra, it has recently been shown that thermal dielectron production rates from the pion gas could be an order of magnitude lower than those from a hadron gas consisting of pions and various resonances [1]. Going beyond simple pion gas considerations is important. Allowing heavier species to partially comprise the system complicates matters since each species might interact among themselves as well as with others. The list of possible processes then becomes quite lengthy. Further complications or uncertainties arise since, with the exception of the pion [2], hadronic form factors are not particularly well known. Reactions which involve an intermediate isoscalar vector meson could contribute to dilepton production and for this reason the mass distribution of produced dileptons is expected to exhibit structure owing to these hadronic resonances.

Observed spectra from heavy-ion collisions will of course be restricted to a time-integrated yield. Temperature (or time) dependent rates are the essential quantity that might be input for models of the time evolution in order to make predictions for overall yields. Rate calculations have been done with various levels of sophistication. In a quest for more accurate knowledge of dielectron production rates we consider some hadronic processes which produce e^+e^- pairs and then compare with spectra calculated previously [1,3]. The particular processes we consider are pseudoscalar and vector reactions of the type $P + V \to V^{I=0} \to e^+e^-$ where P and V are either pions and ρ-mesons or kaons and $K^*(892)$s. The intermediate isoscalar vector hadronic resonances are $\phi(1020), \omega(1390)$ and $\omega(1600)$ for the $\pi\rho$ processes and $\phi(1680)$ for the strange-particle process. Special attention is payed to experimental data on the time-reversed processes in order to constrain or even fix the coupling constants.

Our paper is organized in the following way. In Sect. II we present the basic formalism for the interactions among the hadronic degrees of freedom and the elementary scattering (annihilation) processes. A vector-meson-dominance (VDM) approach will be presented which allows calculation of the basic Feynman diagram for $a+b \to V^{I=0} \to \gamma^* \to e^+e^-$. Within this approach the amplitude for each diagram contains a ratio of the strong-to-electromagnetic coupling constants. Experimental data on cross sections for the time reversed processes $e^+e^- \to a + b$ are shown as compared with model calculations. These are used to fix coupling constants and phases between diagrams. One is really constructing an effective form factor by this prescription. Section III contains the essential details and results for thermal production rates which include effects from these hadronic resonances. The interesting result is that the $\omega(1390)$ and $\phi(1680)$ peaks are visible above the rate from $\pi^+\pi^-$ annihilation and even πa_1 reactions which have recently been shown to be dominant for restricted masses [3]. Finally, in Sect. IV we conclude with some final remarks which essentially stress the importance of appealing to experimental data at some level for the elementary reactions in

future studies. Putting them into calculations on systems of hadronic matter only after such comparison minimizes uncertainty.

II. FORMALISM

After the initial stage of a collision of the type we consider, which may well include a prehadronic or quark-gluon-plasma (QGP) phase, hadronization gives rise to a hot ensemble of the lighter mesons. Within the context of a thermodynamic model this system's composition has recently been studied [4]. The most abundant hadronic species in this scenario are pions, kaons, ρ-mesons and $K^*(892)$ strange vector mesons owing to the large spin-isospin degeneracy of the last two. With temperatures ranging from phase boundary or crossover temperature downward toward the pion mass or lower, where the system ceases interacting, the number densities of these species range from several hundredths to a few tenths per fm^3 [4]. Until freezeout, they interact very strongly. Though binary reactions dominate at these densities, studies of the effect of ternary reactions have been pursued [5]. In this work our aim was to study the relative strength of different lepton pair producing sources and the possible manifestation of some higher-lying resonances. For this, we have chosen a simple thermal environment on purpose. As is well known from the analysis of heavy ion collisions in the intermediate energy regime, nonequilibrium effects might manifest themselves in the final state. A related issue here is the importance of Drell-Yan and $D\bar{D}$ lepton pair signals around the invariant mass region adjacent to the J/ψ [6]. Those are obviously important and should be adressed in a realistic comparison with heavy ion experimental data.

Species can be classified according to their quantum numbers in order to identify the manner with which we model their interactions. Pseudoscalar particles (P) interact with a vector particle (V) in a manner described by the Lagrangian [7]

$$L_{VPP} = g_{VPP}\, V^\mu P \overset{\leftrightarrow}{\partial_\mu} P \tag{2.1}$$

and vectors interact with a pseudoscalar through

$$L_{VVP} = g_{VVP}\, \epsilon_{\mu\nu\alpha\beta}\, \partial^\mu V^\nu \partial^\alpha V^\beta\, P. \tag{2.2}$$

Let two hadrons, call them a and b, scatter in a timelike fashion, i.e. let them annihilate to form a resonant state V—restricted here to neutral vector mesons. It is not entirely clear how it converts itself from a hadronic to an electromagnetic field, but we model the phenomenon using the principle of vector-meson dominance. In practice, it means that the neutral component of the hadronic vector field couples directly to the photon via [8]

$$L_{VA} = \left(\frac{em_V^2}{g_V}\right) V_\mu^{(3)} A^\mu \tag{2.3}$$

where $V^{(3)}$ is the neutral component of the resonant isovector field and A is the electromagnetic field. Using Eqs. (2.1) or (2.2) and (2.3) we construct the general annihilation diagram through a vector resonance V to a virtual or massive photon, which subsequently decays into a lepton pair as shown in Fig 1. This differs from an analogous process of purely electromagnetic exchange because of the presence of the hadronic resonance. Since the effect

of this resonance appears as a function of invariant mass alone, the hadronic dependence of V at the vertex factorizes from the rest of the diagram in Fig. 1 as a form factor times a pointlike electromagnetic process. Vector-meson dominance has been very successful in the areas of hadronic form factors, photoproduction and absorption cross sections, and in the vector meson exchange contributions to πN and NN scattering.

An invariant amplitude for scattering or decay in which the photon couples to the vector meson contains the ratio g_{Vab}/g_V which forces the appearance of the same ratio (squared) in the cross section or decay rate. We will discuss two methods for fixing these quantities. For the case of the $\phi(1020)$ we can fix these coupling constants independently via strong and electromagnetic decays; whereas for the higher excitations presently considered we are forced to use another procedure. First consider the decay $\phi \to \rho\pi$. We calculate its rate to be

$$\Gamma_{\phi\to\rho\pi} = \frac{g^2_{\phi\rho\pi}|\boldsymbol{p}\,|^3}{12\pi} \tag{2.4}$$

where $\boldsymbol{p}$ is the center-of-mass momentum of the decay products. This determines $m^2_\phi g^2_{\phi\rho\pi}/4\pi = 0.29$ when the partial decay rate is taken to be 12.9% of 4.43 MeV. The same expression and numerical conclusions were reached in a recent study of ϕ-meson properties at zero and finite temperature [9]. Next, the electromagnetic decay $\phi \to e^+e^-$ is modeled and computed to be

$$\Gamma_{\phi\to e^+e^-} = \frac{4\pi\alpha^2 m_\phi}{3g^2_\phi}. \tag{2.5}$$

Using the branching fraction $\Gamma_{\phi\to e^+e^-}/\Gamma^{\rm full}_\phi = 3.09\times10^{-4}$, we arrive at the dimensionless vector-dominance coupling constant for the ϕ of $g_\phi = 12.9$.

Since data are not sufficient to allow us to follow this prescription for the other resonances, we instead appeal to the time-reversed hadron production processes

$$e^+e^- \to a + b + \ldots \tag{2.6}$$

We compute the cross sections for $e^+e^- \to \rho\pi$ and for $e^+e^- \to \bar{K}K^*(892)$ which is approximated by $e^+e^- \to K^0_S K^\pm\pi^\mp$. Henceforth $K^*(892)$ will be written just as K^*. The diagrams are shown in Figs. 2a and 2b. The cross section for the process in Fig. 2a is found to be

$$\sigma_{e^+e^-\to\pi\rho}(M) = \frac{4\pi\alpha^2|\boldsymbol{p}\,|^3\,|F_{\pi\rho}(M)|^2}{3M^3} \tag{2.7}$$

where $M = \sqrt{\boldsymbol{p}^2+m^2_\pi} + \sqrt{\boldsymbol{p}^2+m^2_\rho}$ and

$$F_{\pi\rho}(M) = \sum_V \left(\frac{g_{V\pi\rho}}{g_V}\right)\frac{e^{i\varphi_V}m^2_V}{m^2_V - M^2 - im_V\Gamma_V}, \tag{2.8}$$

with the sum running over the three vectors $\phi(1020), \omega(1390)$ and $\omega(1600)$. $\omega(783)$ could also be included in the sum but since it is so far off shell for masses considered here it can safely be neglected. Comparison with experiment constrains the ratios of coupling constants as well as phase angles in Eq. (2.8). The comparison to data is shown in Fig. 3. Details

of the parameters in our model go as follows. For the phases we take $\varphi_\phi = 0$ (without loss of generality one of them can be set to zero), $\varphi_\omega = 5\pi/4$ and $\varphi_{\omega'} = \pi$; while the ratios are taken to be $g_{\omega\pi\rho}/g_\omega = 0.29$ GeV^{-1} and $g_{\omega'\pi\rho}/g_{\omega'} = 0.05$ GeV^{-1}. Note that $g_{\phi\pi\rho}/g_\phi = 0.15$ GeV^{-1} was already fixed by Eqs (2.4–2.5). Notation used here is that ϕ means $\phi(1020)$, ω stands for $\omega(1390)$ and ω' is $\omega(1600)$.

The strange particle process $e^+e^- \to \bar{K}K^*$ approximated by the reaction with the eventual three-body final state is shown in Fig. 2b. Since the decay of K^* is practically entirely into $\pi + K$, these are nearly equivalent. We take a relativistic Breit-Wigner form for the cross section. Computing $\Gamma_{e^+e^-\to\phi'}$ and $\Gamma_{\phi'\to\bar{K}K^*}$, σ can be written as

$$\sigma_{e^+e^-\to\bar{K}K^*}(M) = \frac{\pi\alpha^2\lambda^{3/2}(M^2, m_{\bar{K}}^2, m_{K^*}^2)}{8M^4 m_{\phi'}^2}\,|F_{KK^*}(M)|^2 \tag{2.9}$$

where $\lambda(x,y,z) = x^2 - 2x(y+z) + (y-z)^2$ and

$$F_{KK^*}(M) = \left(\frac{g_{\phi' KK^*}}{g_{\phi'}}\right)\frac{m_{\phi'}^2}{m_{\phi'}^2 - M^2 - i m_{\phi'}\Gamma_{\phi'}}. \tag{2.10}$$

Using value $g_{\phi' KK^*}/g_{\phi'} = 0.19$ GeV^{-1} we generate the curve shown in Fig. 4 compared with experiment. Also shown is the result from a fully microscopic calculation of the exact diagram of Fig. 2b whose cross section involves integration over full three-body phase space. Given the forms of the interactions written in Eqs. (2.1) and (2.2), the model form of the cross section is well defined. It is presented as the dashed curve. The same ratio of coupling constants is used in both approaches.

III. THERMAL PRODUCTION RATES

Hadrons in this hot reaction zone are assumed to have their momenta thermally distributed. Then the differential rate at which they scatter, i.e. the differential rate at which hadrons annihilate to create an e^+e^- pair of invariant mass M can be written as

$$\begin{aligned}\frac{dR}{dM^2} = \mathcal{N}\int \frac{d^3p_a}{2E_a(2\pi)^3}\frac{d^3p_b}{2E_b(2\pi)^3}\frac{d^3p_+}{2E_+(2\pi)^3}\frac{d^3p_-}{2E_-(2\pi)^3} f(E_a)f(E_b) \\ \times(2\pi)^4|\,\overline{\mathcal{M}}\,|^2\delta^4(p_a + p_b - p_+ - p_-)\delta\left(M^2 - (p_+ + p_-)^2\right)\end{aligned} \tag{3.1}$$

where f is the Bose-Einstein distribution and $\mathcal{N}$ is an overall degeneracy factor. With the aid of the δ functions some of the phase space can be reduced analytically. We integrate the rest numerically. The absolute square of the scattering amplitude for $\pi\rho \to e^+e^-$ (initial spin averaged and final spin summed) is

$$|\,\overline{\mathcal{M}}\,|^2 = \frac{4e^4}{3}\frac{|F_{\pi\rho}(M)|^2}{M^4}\,\epsilon_{\mu\nu\alpha\beta}\,\epsilon_{\kappa\lambda\sigma\tau}\,q^\mu q^\kappa p_\rho^\alpha p_\rho^\sigma\left(-g^{\beta\tau}\right)\left[p_+^\nu p_-^\lambda + p_-^\nu p_+^\lambda - g^{\nu\lambda}(p_+\cdot p_-)\right] \tag{3.2}$$

where where $q^\mu = p_+^\mu + p_-^\mu$ so that $q^2 = M^2$ and finally, where the form factor is given by Eq. (2.8).

For later convenience it is useful to compute the cross section arising from this squared amplitude. We get

$$\sigma_{\pi\rho\to e^+e^-}(M) = \frac{2\pi\alpha^2 \left|F_{\pi\rho}(M)\right|^2 \lambda^{1/2}(M^2, m_\pi^2, m_\rho^2)}{9M^2}. \tag{3.3}$$

Then the thermal rate can be written

$$\frac{dR}{dM^2} = \frac{\mathcal{N}}{2(2\pi)^4} \int dE_\pi dE_\rho f(E_\pi) f(E_\rho) \sigma(s) \lambda^{1/2}(s, m_\pi^2, m_\rho^2) \Theta(\chi) \tag{3.4}$$

where

$$\chi = 4\boldsymbol{p}_\pi^2 \boldsymbol{p}_\rho^2 - \left(m_\rho^2 + m_\pi^2 - s + 2E_\rho E_\pi\right)^2. \tag{3.5}$$

Notice that s and M^2 have been used interchangeably. The integration required by Eq. (3.4) can of course be done numerically for arbitrary distributions. However, assuming Boltzmann distributions for the mesons it is a straigtforward exercise to perform the integration and arrive at the much simpler expression for the rate

$$\frac{dR}{dM^2} = \mathcal{N} \frac{T}{32\pi^4 M} K_1(M/T) \lambda(s, m_\pi^2, m_\rho^2) \sigma(s) \tag{3.6}$$

where K_1 is the first modified Bessel function. Making the replacements $m_\rho \to m_{K^*}$, $m_\pi \to m_K$ and using the appropriate degeneracy $\mathcal{N}$, one arrives at the thermal rate for lepton pair emission through $\bar{K}K^* + \text{c.c.} \to e^+e^-$.

Results at 150 MeV temperature presented in Fig. 5. We have compared rates which were integrated numerically starting from Bose-Einstein distributions to those computed using classical distributions written finally as Eq. (3.6). Since there is no final-state hadron in these reactions and therefore no Bose-enhancement effects, the classical distributions are more than adequate. For comparison purposes we also include the results for $\pi^+\pi^-$ annihilation [1] and for πa_1 reactions from Ref. [3] which were concluded to be dominant for masses above m_ϕ. The importance of the excitations of $\omega(1390)$ and $\phi(1680)$ are immediate: they are visible above the tail of the $\pi^+\pi^-$ annihilation and even above the πa_1 results. One last figure is shown (Fig. 6) where a temperature of 200 MeV is used. Our conclusions are independent of the temperature.

IV. FINAL REMARKS

Timelike photons are observed to have a strong affinity for neutral hadronic fields. This observation is captured in the current field identity [13] which is a consequence of the VMD hypothesis. These photons, observed as lepton pairs, exhibit resonant structure when the observed particles are projected onto a mass spectrum. One understands these peaks within vector-meson dominance to be manifestations of hadronic form factors. Our study suggests that in order to improve knowledge of dielectron production rates from hot hadronic matter, at least for dielectron masses ranging from m_ϕ to $m_{J/\psi}$, form factors for hadrons other than just the pion must be considered. We show only two examples of additional structure in the mass spectrum—there may well be more surprises.

World data on electron-positron annihilation into hadrons is quite extensive at higher energies but is unfortunately not as complete for lower energies. However, that which does

exist should be exploited to its fullest potential. In our study we have constructed effective form factors $|F_{\pi\rho}(M)|^2$ and $|F_{KK^*}(M)|^2$ in the mass range 1–2.5 GeV. After doing so, we have compared each elementary process with known data before using them in a thermal calculation on the extended system of interacting hadrons. Higher excitations of the ω and ϕ, namely $\omega(1390)$ and $\phi(1680)$, were found to be visible in the mass distribution of the dilepton production rate above the hadronic production mechanisms previously considered.

ACKNOWLEDGMENTS

K.H. acknowledges support from the National Science Foundation under grant number PHY-9403666 and wishes to thank the Physics Department at McGill University for hospitality during a visit in May 1994 when initial stages of this work were discussed. C.G. acknowledges support from the Natural Sciences and Engineering Research Council of Canada, the FCAR of the Québec Government and a NATO Collaborative Research Grant.

REFERENCES

* electronic address: haglin@theo03.nscl.msu.edu
† electronic address: gale@hep.physics.mcgill.ca

[1] C. Gale and P. Lichard, Phys. Rev. D **49**, 3338 (1994).
[2] DM2 Collaboration, Phys. Lett. **B 220**, 321 (1989).
[3] C. Song, C.M. Ko and C. Gale, Phys. Rev. D **50**, R1827 (1994).
[4] K. Haglin and S. Pratt, Phys. Lett. **B 328**, 255 (1994).
[5] P. Lichard, Phys. Rev. D **49**, 5812 (1994).
[6] M. C. Abreu *et al.*, Nucl. Phys. **A566**, 77c (1994); and references therein.
[7] U.-G. Meissner, Phys. Rep. **161**, 213 (1988).
[8] J.J. Sakurai, Ann. Phys. (N.Y.) **11**, 1 (1960).
[9] K.L. Haglin and C. Gale, Nucl. Phys. **B421**, 613 (1994).
[10] V.M. Aulchenko *et al.*, Novosibirsk Preprint 86–106 (1986); A. Donnachie and A.B. Clegg, Z. Phys. C **42**, 663 (1989).
[11] R. Baldini–Ferroli in Proc. Had. Phys. at Intermediate Energy, T. Bressani, B. Menetti, and G. Pauli (eds.) Amsterdam, New York, Elsevier (1987); A. Donnachie and A.B. Clegg, Z. Phys. C **42**, 663 (1989).
[12] F. Mane, *et al.*, Phys. Lett. **B 112**, 179 (1982).
[13] N. Kroll, T.D. Lee and B. Zumino, Phys. Rev. **157**, 1376 (1967).

FIGURES

FIG. 1. General annihilation diagram of two hadrons a and b to a lepton pair. The process goes through a vector hadronic resonance V and by vector-meson dominance, goes directly to a virtual photon.

FIG. 2. Annihilation of e^+e^- into $\pi\rho$ through any of three isoscalar vectors $\phi(1020)$, $\omega(1390)$ and $\omega(1600)$ in (a) and in (b) $e^+e^- \to K_S^0 K^\pm \pi^\mp$.

FIG. 3. Cross section for $e^+e^- \to \pi\rho$ as computed within the model described in the text as compared with experimental data from Ref. [10,11].

FIG. 4. Cross section for $e^+e^- \to \bar{K}K^*$ described by the Breit-Wigner form presented in the text (solid curve), results of a microscopic calculation for the full process (dashed curve) and finally, experimental data for the reaction $e^+e^- \to K_S^0 K^\pm \pi^\mp$ from Ref. [12].

FIG. 5. Thermal production rate at $T = 150$ MeV from $\pi\rho$ (solid curve) processes, $\bar{K}K^*$+c.c. (dotted curve), $\pi^+\pi^-$ annihilation from Ref. [1] (dot-dash curve) and finally, πa_1 process as calculated in Ref. [3] (dashed curve).

FIG. 6. Same as Fig. 5 except using $T = 200$ MeV.

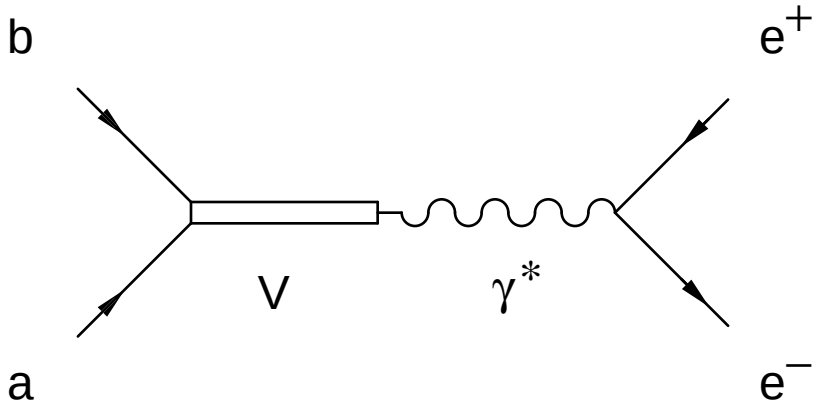

Figure 1

K. Haglin and C. Gale, ‘‘Higher Excitations of omega and phi in Dilepton Spectra’’

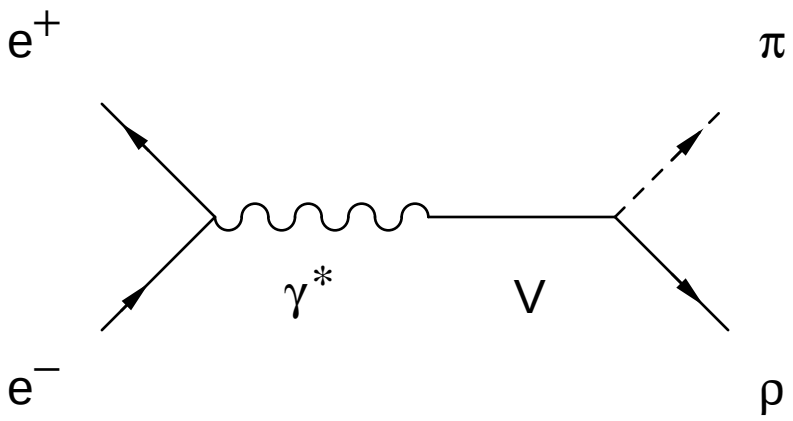

(a)

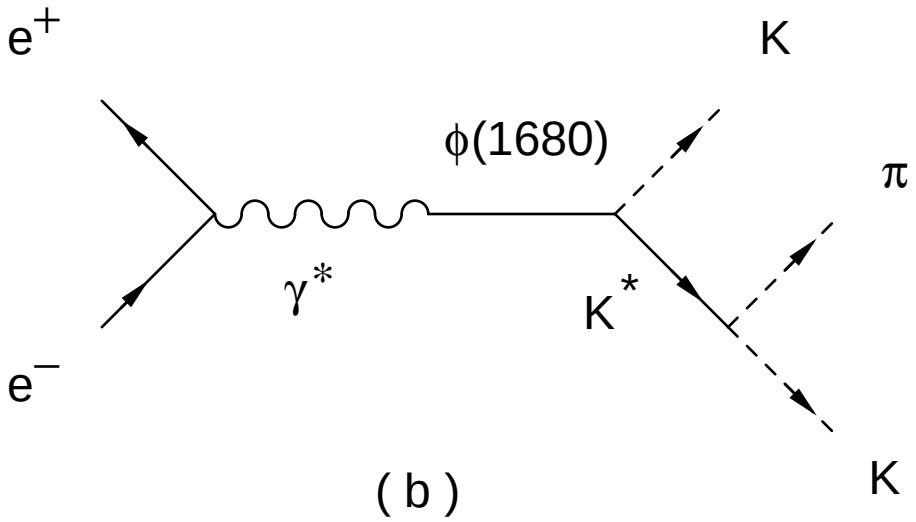

(b)

Figure 2

K. Haglin and C. Gale, ‘‘Higher Excitations of omega and phi in Dilepton Spectra’’

K. Haglin and C. Gale, ‘‘Higher Excitations of omega and phi in Dilepton Spectra’’ - Figure 3

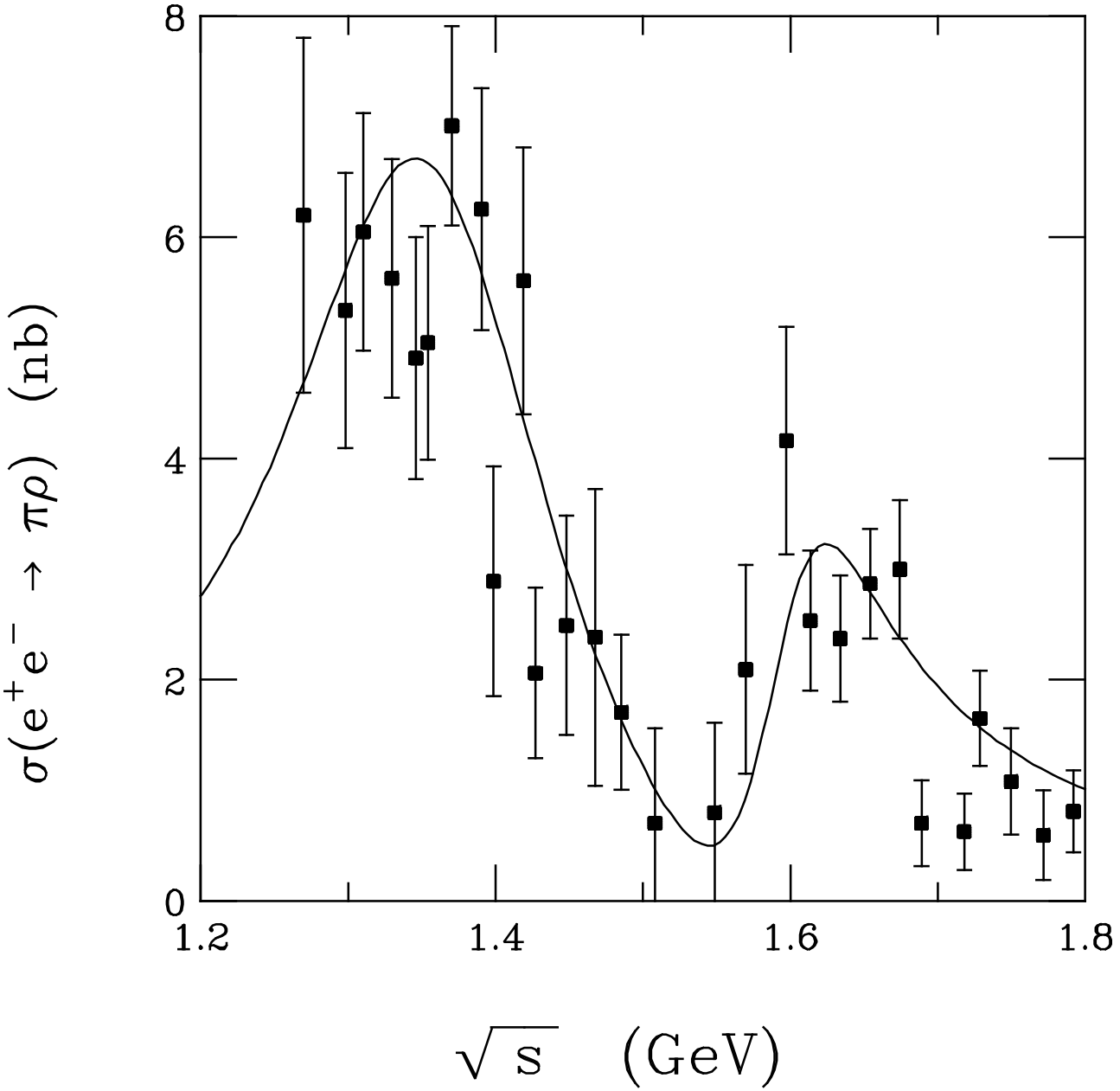

K. Haglin and C. Gale, ‘‘Higher Excitations of omega and phi in Dilepton Spectra’’ - Figure 4

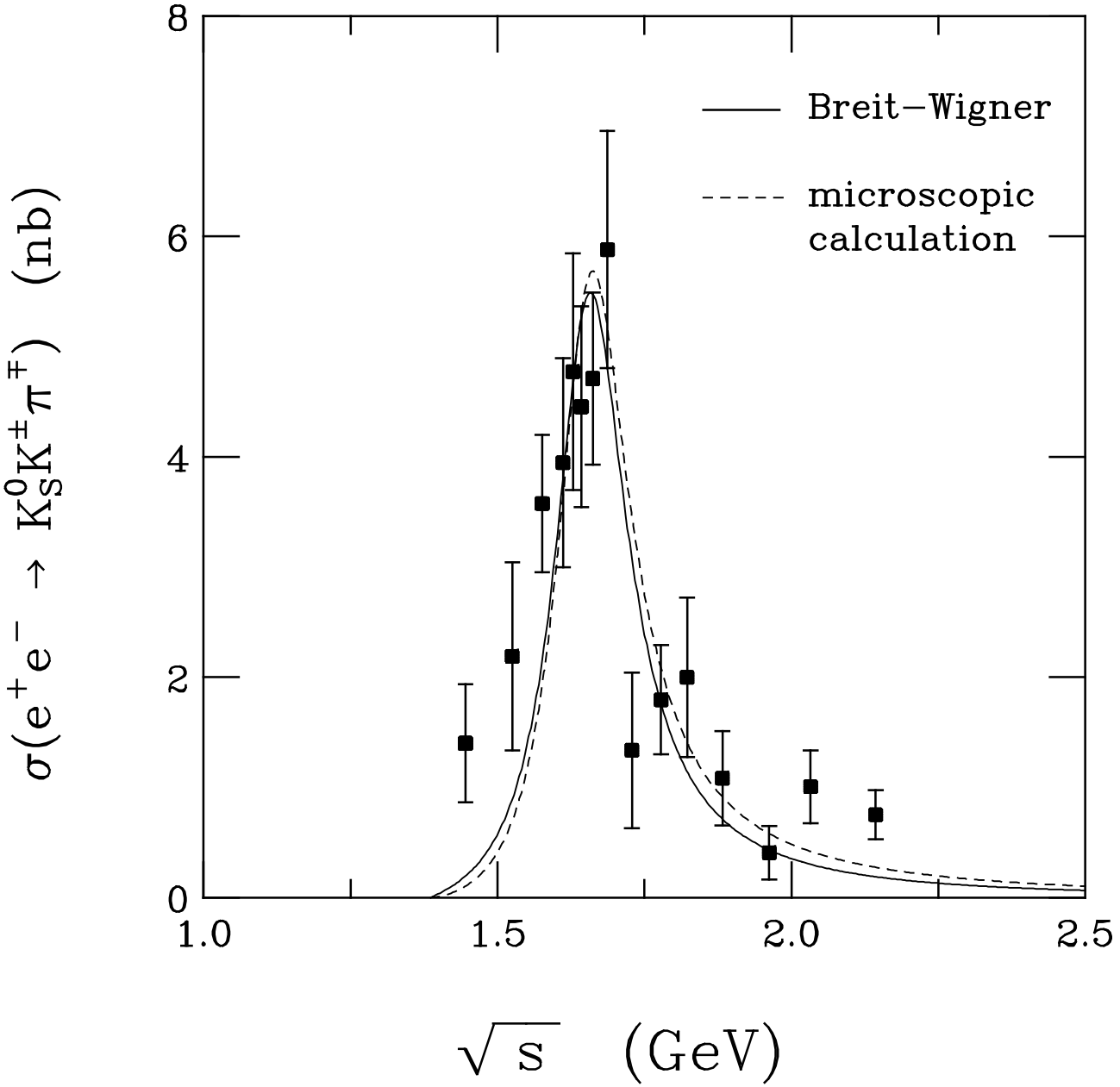

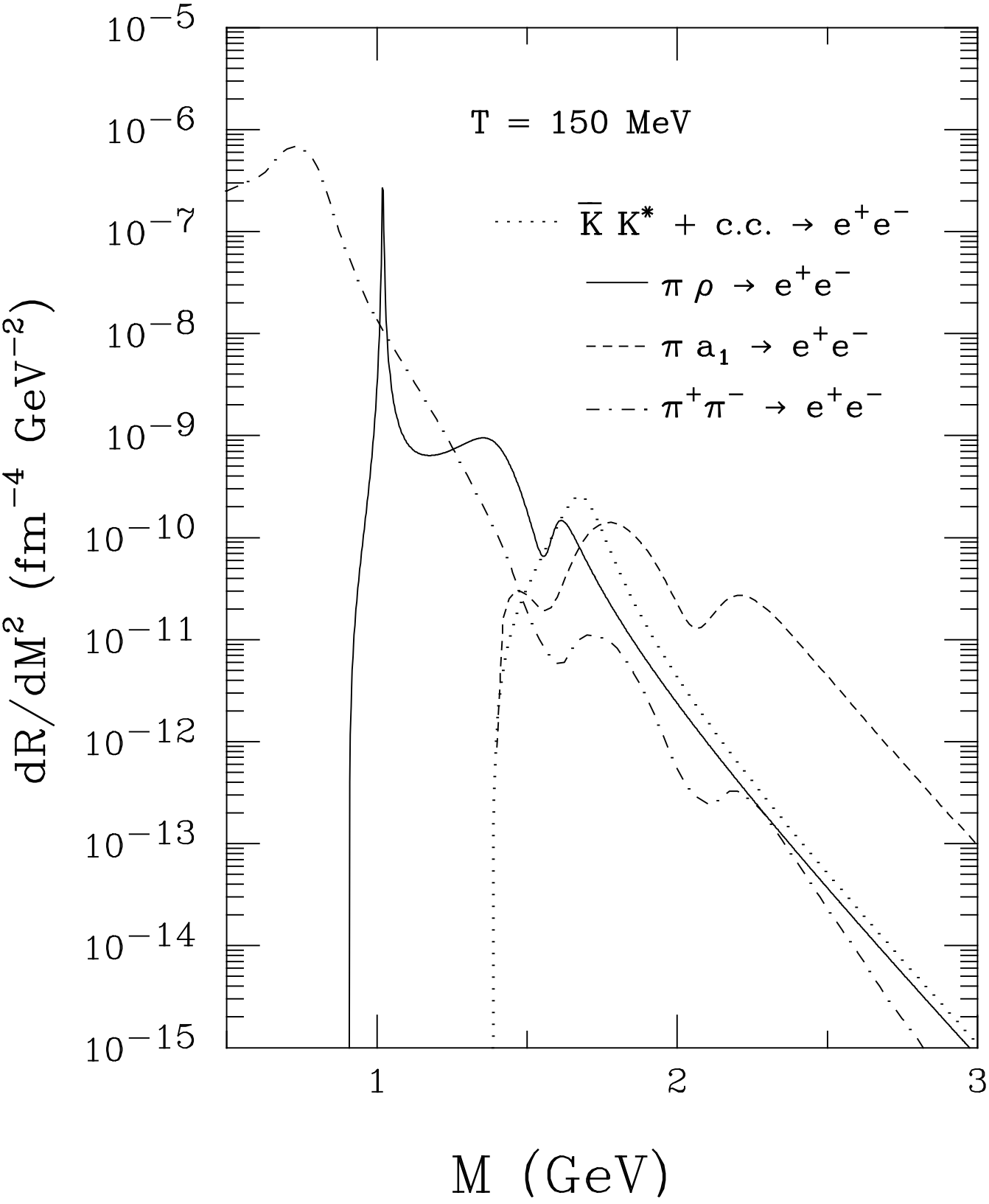

K. Haglin and C. Gale, ‘‘Higher Excitations of omega and phi in Dilepton Spectra’’ - Figure 5

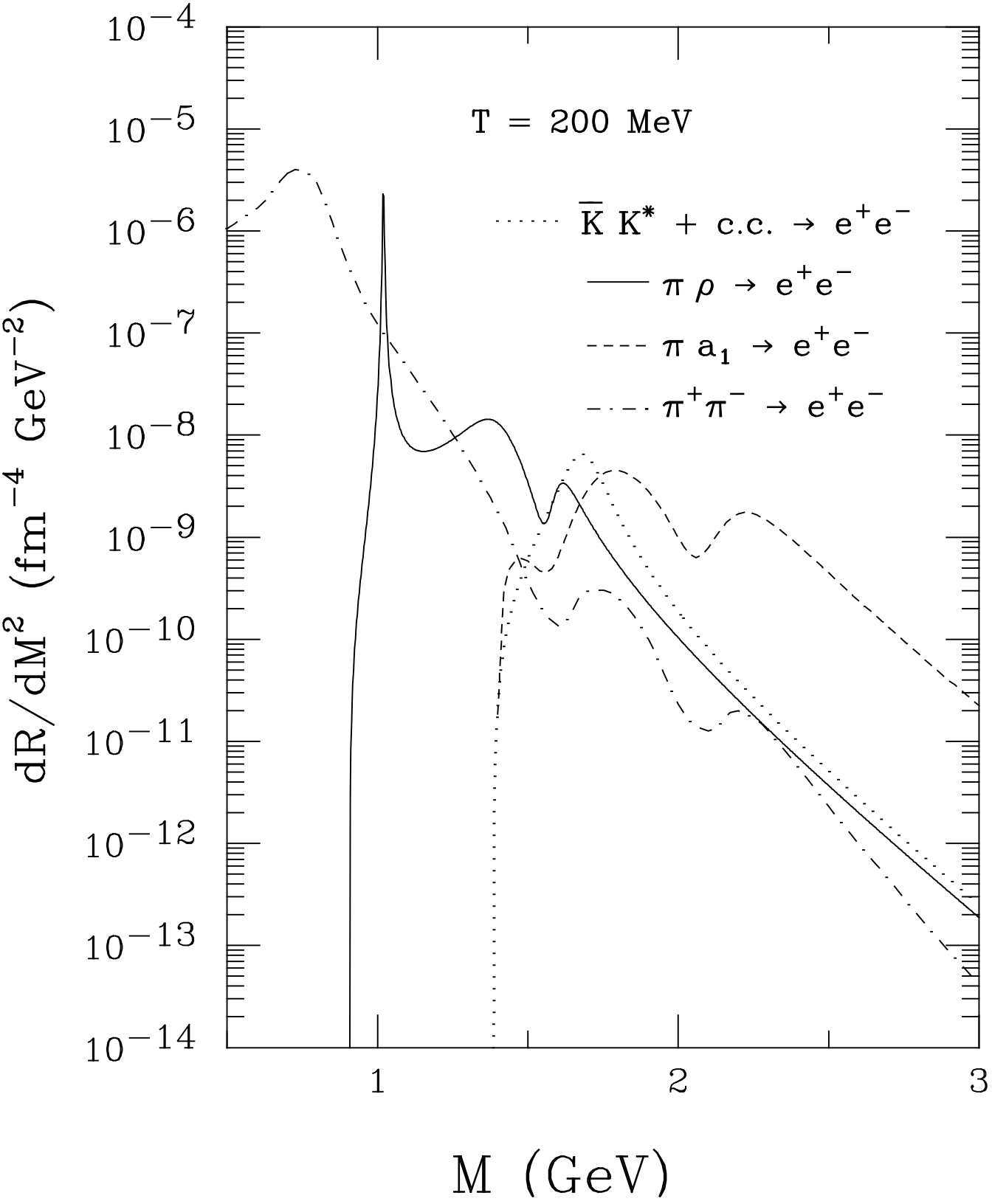

K. Haglin and C. Gale, ‘‘Higher Excitations of omega and phi in Dilepton Spectra’’ - Figure 6